Frequency-Space-Polarization on UWB MIMO Performance for Body Area Network Applications

Wei-Ju Chang, Jenn-Hwan Tarng, *Senior Member, IEEE*, and Szu-Yun Peng

***Abstract*—This letter experimentally investigates the performance of ultrawideband (UWB) radio technologies with multiple-input–multiple-output (MIMO) antennas for body area network (BAN) applications. Effects of array spacing, antenna polarization, bandwidth and propagation on UWB-MIMO channel capacity are analyzed. The key finding here is to that in BAN the MIMO channel capacity is mainly determined by the power imbalance between subchannels compared to the sub channel correlation for both spatial array and polar array. For spatial array, the measured results show that the MIMO channel capacity is decreased when the array spacing is increased, despite the spatial correlation coefficient is decreased. This phenomenon is different from that in wide area networks (WAN) and wireless local area networks (WLAN). It is because that power difference among elements of the spatial array is significant in BAN short-range communications compared to that in WAN and WLAN. For polar array, the achievable channel capacity is lower than that of the spatial array in line-of-sight (LOS) conditions due to high cross-polarization discrimination. Furthermore, the MIMO capacity is slightly dependent on the environments due to dominance of human body effect. It is also found that the MIMO channel capacity decreased with frequency or bandwidth.**

***Index Terms*—Body area networks (BANs), multiple-input–multiple-output (MIMO), radio propagation, ultrawideband (UWB).**

I. Introduction

USING wireless sensors around the body to monitor health information is a promising new application made possible by recent advances in ultra low power technology [1]. The large diversity and potential of these applications makes it an exciting new research direction in wireless communications. The gain of interest for body area networks (BAN) is confirmed by the IEEE 802.15.4a standardization committee. This group is mandated to develop a physical layer based on the promising ultrawideband (UWB) radio technologies to provide energy- efficient data communications.

Manuscript received March 16, 2008; revised April 29, 2008. First published May 16, 2008; current version published December 30, 2008. This work was supported by the National Science Council of Republic of China under Contract numbers NSC-93-2752-E-002-009-PAE, NSC 93-2752-E-009-003-PAE and NSC 94-2213-E-009-070.

W.-J. Chang is with the Department of Communication Engineering, National Chiao-Tung University, Hsin-Chu, 301 Taiwan, China, and also with Chunghwa Telecom Laboratories, Taoyuan, 326 Taiwan, China (e-mail: wjcha@cht.com.tw).

J.-H. Tarng and S.-Y. Peng are with the Department of Communication Engineering, National Chiao-Tung University, Hsin-Chu, 301 Taiwan, China (e-mail: j4t@mail.nctu.edu.tw; sypeng.iic94g@nctu.edu.tw).

Color versions of one or more of the figures in this letter are available online at http://ieeexplore.ieee.org.

Digital Object Identifier 10.1109/LAWP.2008.2000640

In addition to UWB, multiple-input–multiple-output (MIMO) technologies have attracted great interest for broadband wireless communications due to its potential to provide channel capacity gain without additional bandwidths. Its use in wide area networks (WAN) and wireless local area networks (WLAN) has been extensively studied [2]. However, to date, the use of MIMO for BAN has not been considered.

To our knowledge, measurements of UWB-MIMO channels for BAN were presented in few literatures [3], [4] so far. In [3], MIMO channel characteristics were investigated through measurements with two on-body dual-polar antennas. In the experiment, the array spacing is fixed to one wavelength and the frequency bandwidth is 120 MHz, which is not satisfied the bandwidth requirement of UWB technologies. In [4], the spatial correlation in frequency and delay domains were extracted from channel measurements on the human torso in band of 3–10 GHz. In the experiment, only co-polarized transmitting and receiving antennas are used. Analysis of the MIMO channel capacity is not presented in the literature.

In this letter, performance of UWB-MIMO for BAN channel capacity improvements is investigated through extensively measurements for both spatial and polar antenna arrays. In our experiments, channel frequency responses were measured in the frequency ranges of 3–10 GHz that covers the whole UWB band. The array spacing is varied from 3 cm to 12 cm. Furthermore, vertical- and horizontal-polarized receiving antennas were used to investigate performance of cross- polarized antennas. From the measured channels, effects of propagation condition, bandwidth, array spacing, and antenna polarization on UWB-MIMO channel capacity are analyzed.

II. Measurement Setup and Sites

In our study, the frequency domain measurement technology to perform UWB BAN indoor channel sounding is adopted. An Agilent 8719ET vector network analyzer (VNA) was used to record the variation of 801 complex tones between the transmitting and receiving antennas across 3–6 GHz, 6–10 GHz and 3–10 GHz frequency ranges, respectively. Here, the UWB antenna is a planar binominal curved monopole antenna [5]. Fig. 1 shows the measured antenna return loss versus frequency. As shown, the return loss is below -10 dB from 3 to 10 GHz.

Since our measurements were performed at night, therefore, the measured channel is nearly time-invariant. MIMO channels are formed by collecting multiple single-input-single-output (SISO) channel responses. As shown in Fig. 2, the transmitting antenna is moved to 5 fixed subpoints with 3-cm spacing. Meanwhile, for each transmitting antenna subpoint, the receiving antenna is moved to 5 fixed subpoints with 3-cm spacing. In

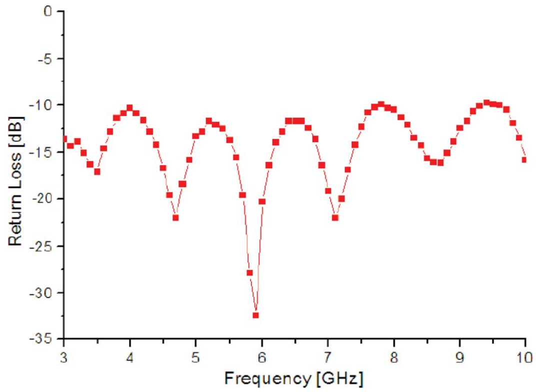

Fig. 1. Measured antenna return loss versus frequency.

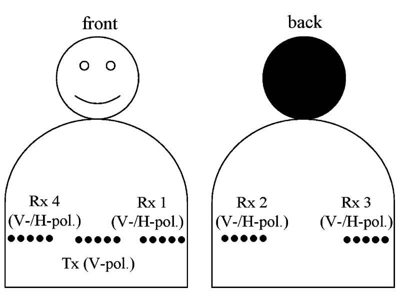

Fig. 2. The locations of Tx and Rx antennas for MIMO measurements.

addition, at each receiving antenna subpoint, channel responses were measured for both the vertical- and horizontal-polarized receiving antennas. For each environment, MIMO channel responses are measured at four receiving antenna positions (Rx 1-4) as shown in Fig. 2, while the transmitting antenna (Tx) is always placed on the front of the body. Therefore, in our experiment, $5 \times 5 \times 2 \times 4$ SISO channel measurements were performed at each site. Here, the MIMO channels between Tx and Rx 1-4 are denoted as MIMO_1-4, respectively. The transmitting and receiving arrays are under LOS conditions for MIMO_1 and MIMO_4 cases, while other cases are NLOS conditions.

UWB-MIMO BAN propagation experiments are performed at Microelectronics and Information System Research Center (MISRC) in the National Chiao-Tung University, Hsinchu, Taiwan. Fig. 3(a) shows the floor layouts of the measurement sites, Sites A and B, at the lobby of 2nd floor of MISRC. In Sites A and B, measurements were performed at the center and side of the lobby, respectively, to understand the effect of reflected waves caused by the sidewall. Fig. 3(b) shows the layout of Site C, laboratory #810 at 8th floor of MISRC. Since there are many computers and tables in laboratory #810, measurement results in this site are helpful to understand the effects of local scatters to UWB-MIMO BAN channels.

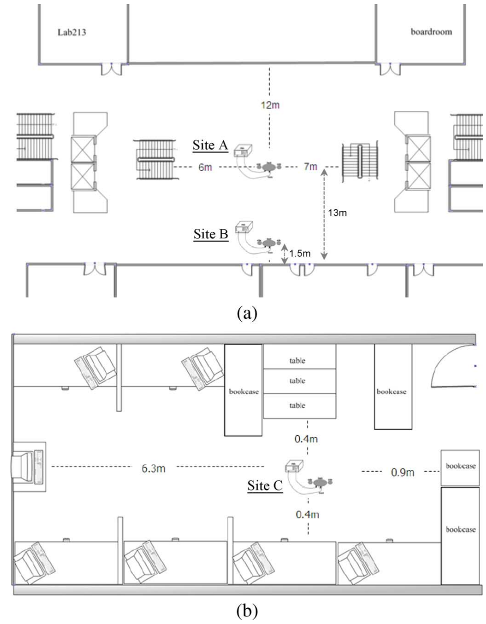

Fig. 3. Floor layouts of measurement sites. (a) Sites A and B and (b) Site C.

III. UWB MIMO Channel Capacity

Given an UWB-MIMO system with M transmitting elements and N receiving elements, the UWB-MIMO channel capacity (bits/sec/Hz) is given by [6]

$$C = \frac{1}{N_f} \sum_{f=1}^{N_f} \log_2 \left[\det \left(I_N + \frac{\rho}{M} H(f) H^*(f) \right) \right] \quad (1)$$

where N_f is frequency component f, which is equal to 801 in our measurements. $H(f)$ is the normalized frequency-dependent transfer matrix, which is obtained by normalizing the measured transfer matrix to remove the effect of path loss and is given by (2), $*$ denotes the complex conjugation operation, and ρ is the average SNR over the entire bandwidth. It is noted that $\rho = 20$ dB is given to calculate the UWB-MIMO capacity in this letter

$$H(f) = \hat{H}(f) \Bigg/ \sqrt{\sum_{f=1}^{N_f} \left\| \hat{H}(f) \right\|_F^2} \quad (2)$$

where $\hat{H}(f)$ is the measured transfer matrix.

IV. Observations and Discussions

A. Propagation Condition

Table I shows the 2×2 MIMO channel capacity for frequency band of 3–10 GHz. Here, both the array spacing at transmitting and receiving side are equal to 3 cm, i.e., around 0.45 times of wavelength of the center frequency. It is found that channel capacities of MIMO_2 and MIMO_3 cases are greater than that of MIMO_1 and MIMO_4 cases. It is because

TABLE I
THE MEASURED 2 × 2 MIMO CHANNEL CAPACITY FOR FREQUENCY BAND OF 3–10 GHz

Measurement Site	MIMO_1	MIMO_2	MIMO_3	MIMO_4
Site A	9.19	10.30	10.11	9.18
Site B	9.69	10.42	10.20	9.89
Site C	9.78	10.24	10.56	9.71

TABLE II
THE MEASURED 2 × 2 MIMO CHANNEL CAPACITY AT SITE C

Frequency Band	MIMO_1	MIMO_2	MIMO_3	MIMO_4
3-6 GHz	10.85	11.07	11.24	10.70
6-10 GHz	10.27	10.72	11.04	10.10
3-10 GHz	9.78	10.24	10.56	9.71

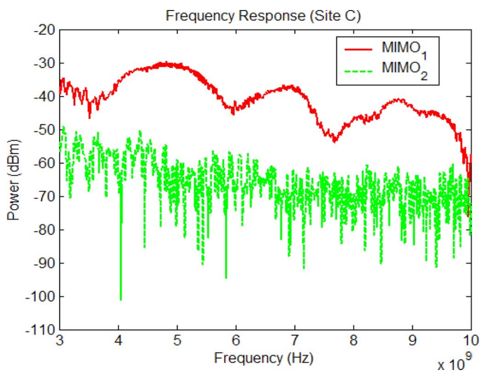

Fig. 4. One subchannel frequency response at Site C.

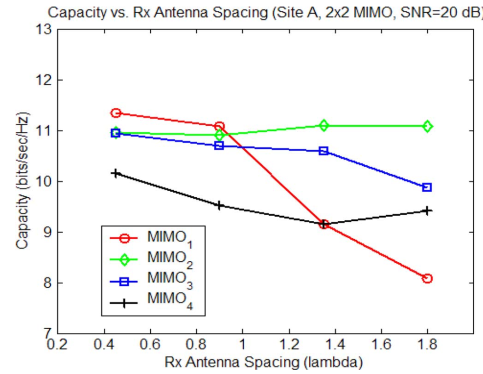

Fig. 5. MIMO channel capacities versus receiving array spacing at Site A.

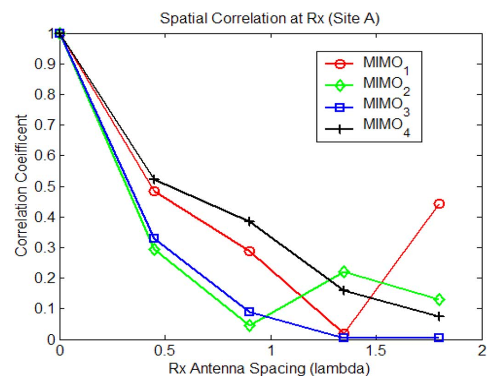

Fig. 6. Spatial correlation coefficients versus receiving array spacing at Site A.

that MIMO_2 and MIMO_3 cases are NLOS situations of rich multipath, which leads to lower correlation among subchannels than those of MIMO_1 and MIMO_4 cases. For example, the average correlation coefficient for 3-cm array spacing is equal to 0.6129, 0.3859, 0.1883 and 0.6216 for MIMO_1-4, respectively, at Site A. It is noted that, similar results were found at Sites B and C.

Table I also shows that the channel capacity is slightly dependent of the measurement sites. For MIMO_1 and MIMO_4 cases, it is because that the body-diffracted path is much strong compared to the multipath caused by scatterers inside the building. For MIMO_2 and MIMO_3 cases, since the transmitting and receiving arrays are under NLOS condition, the correlation between subchannels is low even in Site A, the open space environment. Therefore, the large number of reflected multipath components of Site B and Site C does not give significant contribution on MIMO channel capacity for MIMO_2 and MIMO_3 cases.

B. Bandwidth

Table II shows the measured channel capacity versus frequency band at Site C. Here, the number of array elements is 2×2, and the array spacing is 3 cm. It is found that the MIMO channel capacity decreased with frequency or bandwidth. It is because the receiving power is decreased when the frequency band is increased, which can be found in Fig. 4. For UWB MIMO, the channel capacity is equal to the average of the multiple narrowband channel capacity. Therefore, high frequency components do not give significant contribution to the channel capacity due to its low power.

C. Array Spacing

Fig. 5 shows the 2×2 MIMO channel capacity versus receiving array spacing at Site A. Here, the measured bandwidth is in the range of 3 to 6 GHz. From this figure, it is found that the MIMO channel capacity is decreased when the receiving array spacing is increased for most of the MIMO channels. This phenomenon is different from the result observed in WANs and WLANs. For MIMO channels, the capacity is dependent on the correlations among subchannels and power distribution of received subchannels. It reaches its maximum value when these subchannels are uncorrelated and are of equal mean power. The following two figures may illustrate the mechanism to yield the result shown in Fig. 5.

Fig. 6 shows the spatial correlation coefficient versus receiving array spacing at Site A. It is found that the spatial correlation coefficient is decreased when the array spacing is increased, which has different trend as that shown in Fig. 5.

Fig. 7 shows the maximum power difference among the subchannels versus the array spacing. It is found that the maximum value of the power difference between any two subchannels is increased when the array spacing is increased. Therefore, some subchannels with small-received power do not contribute to the MIMO channel capacity even when they are uncorrelated to one another. It shows the reason why the MIMO channel capacity of BAN is decreased when the array spacing is increased. In other words, increasing of the MIMO capacity by increasing of array spacing does not work in the BAN despite the spatial correlation coefficient is decreased. It is noted that similar results can be found in Sites B and C.

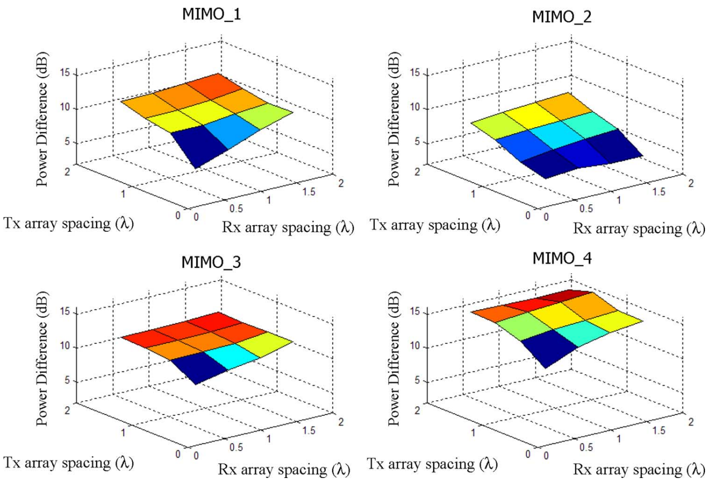

Fig. 7. Maximum value of the power differences between any two subchannels versus receiving and transmitting array spacing at Site A.

TABLE III
THE MEASURED 2 × 2 MIMO CHANNEL CAPACITY OF THE POLAR ARRAY AND THE SPATIAL ARRAY AT SITE C

Configuration of array (Tx / Rx)	Rx Array Spacing	MIMO_1	MIMO_2	MIMO_3	MIMO_4
Polar array: V-V / V-H	0	8.17	10.68	10.71	9.13
Spatial array: V-V / V-V	0.45 λ	10.85	11.07	11.24	10.70
	0.90 λ	9.99	10.56	10.57	9.99
	1.35 λ	9.28	10.19	10.39	8.98
	1.80 λ	8.56	9.96	10.04	9.24

D. Antenna Polarization

Table III shows the 2 × 2 MIMO channel capacity of the polar array and the spatial array at Site C. Here, the measured bandwidth is in the range of 3 to 6 GHz. The polar array is composed of two co-polarized transmitting antennas with spacing of 3 cm and two co-located cross-polarized receiving antennas. It is found that the channel capacity of the polar array is similar to that of the spatial array for MIMO_2 and MIMO_3 cases. However, in MIMO_1 and MIMO_4 cases, the channel capacity of the polar array is lower than that of the spatial array. It is because that the contribution of the cross-polarized subchannel is insignificant due to the high cross polarization discrimination in the near-LOS condition as shown in Fig. 8(a) where the received power of the V/V case is much larger than that of the V/H case. However, in the NLOS situation, the cross-polarized subchannel becomes significant due to the same order of magnitude of the multi-path components. Therefore, magnitude of the received power of the V/V case is similar to that of the V/H case, which is observed in Fig. 8(b). It means that, only in the NLOS conditions, the device compactness is achieved by using the polar array without sacrifice of channel capacity compared to the spatial array.

V. CONCLUSION

UWB-MIMO performance has been characterized experimentally in BAN channels for spatial and polar antenna arrays.

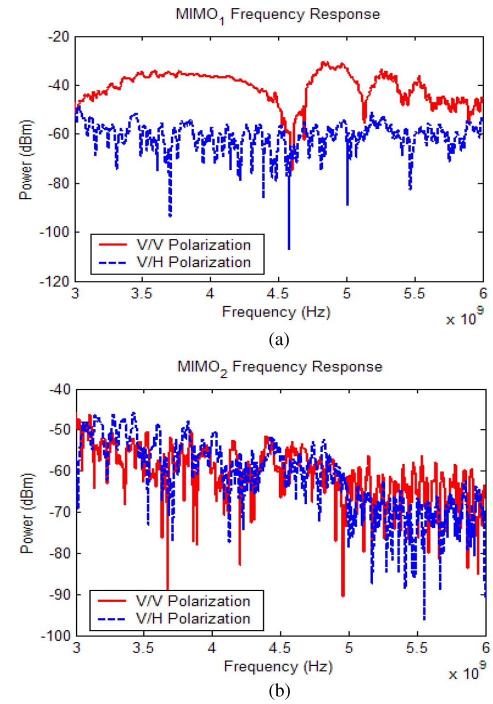

Fig. 8. Received power of V/V or V/H link versus frequency at Site C for (a) MIMO_1 (LOS) and (b) MIMO_2 (NLOS).

For spatial array, the measured results show that MIMO channel capacity is decreased when the array spacing is increased, despite the spatial correlation coefficient is decreased. To achieve maximum channel capacity, the array spacing of spatial array should not be larger than one wavelength. For polar array, it is confirmed that the device compactness can be achieved without sacrifice channel capacity compared to the spatial array in NLOS conditions. However, in LOS conditions, the achievable channel capacity of the polar array is lower than that of the spatial array. Furthermore, MIMO channel capacity is slightly dependent on the environments due to dominance of human body effect. It is also found that the MIMO channel capacity decreased with frequency or bandwidth.

REFERENCES

[1] B. Gyselinckx, C. Van Hoof, and S. Donnay, "Body area networks, the ascent of autonomous wireless microsystems," presented at the Int. Symp. on Hardware Technol. Drivers of Ambient Intelligence, Veldhoven, The Netherlands, Dec. 9–10, 2004.

[2] A. J. Paulraj, D. A. Gore, R. U. Nabar, and H. Bölcskei, "An overview of MIMO communications—A key to gigabit wireless," *Proc. IEEE*, vol. 92, no. 2, pp. 198–218, 2004.

[3] D. Neirynck, C. Williams, A. Nix, and M. Beach, "Exploiting multiple-input multiple-output in the personal sphere," *IET Microw. Antennas Propag.*, vol. 1, no. 6, pp. 1170–1176, 2007.

[4] S. V. Roy, C. Oestges, F. Horlin, and P. De Doncker, "Ultra-wideband spatial channel characterization for body area networks," in *Proc. 2nd Eur. Conf. on Antennas Propag.*, 2007, pp. 1–5.

[5] C. W. Lin, W. H. Lo, R. H. Yan, and S. J. Chung, "Planar binomial curved monopole antennas for ultrawideband communication," *IEEE Trans. Antennas Propag.*, vol. 55, no. 9, pp. 2622–2624, Sep. 2007.

[6] A. F. Molisch, M. Steinbauer, M. Toeltsch, E. Bonek, and R. S. Thoma, "Capacity of MIMO systems based on measured wireless channels," *IEEE J. Sel. Areas Commun.*, vol. 20, no. 3, pp. 561–569, 2002.